

Modifications in Thermal and Anticorrosive Characteristics of Haemoglobin-Doped Polyindole

Komal Khati ^{1,2}

¹ Department of Higher Education, Govt. of Uttarakhand, Radhey Hari Govt. P.G. College Kashipur, Kashipur 244 713, India; komal.chem89@gmail.com; Tel. +91-9012718895

² G.B. Pant University of Agriculture & Technology, Pantnagar 263 145, India

† Presented at the 26th International Electronic Conference on Synthetic Organic Chemistry; Available online: <https://ecsoc-26.sciforum.net>.

Abstract: A method of doping of Haemoglobin (Hb) into Polyindole (PIN) was developed to accomplish the haemoglobin polyindole composite (HPC) with improved electrochemical performance and maintained thermal stability. The scheme of doping was accomplished through cationic surfactant assisted dilute polymerization of indole (0.12 mol dL^{-1}) in the presence of ferric chloride oxidant ($1.85 \times 10^{-2} \text{ mol dL}^{-1}$) augmentation with indispensable weight of Hb (1%; *w/w*). The formation of HPC was ascertained through scanning electron microscopy (SEM), thermogravimetric-differential thermal analysis-differential thermogravimetry (TG-DTA-DTG) and electrochemical impedance spectra (EIS). Working electrode was derived from PIN and HPC in the presence of sulfonated polysulphone binder in graphite matrix. The specific capacitance ($C_s \text{ Fg}^{-1}$) of PIN and respective HPC (1% *w/w*) electrodes has been 21.60 and 39.40 respectively. In order to have further imminent into the consequence of Hb on the stability, the SEM images have been recorded before and after polarization experiments. The rendered enhanced impact, thermal stability and remarkable potential as anticorrosive coating.

Keywords: polyindole; haemoglobin; specific capacitance; thermal stability; anticorrosive

Citation: Khati, K. Modifications in Thermal and Anticorrosive Characteristics of Haemoglobin-Doped Polyindole. *Chem. Proc.* **2022**, *4*, x. <https://doi.org/10.3390/xxxxx>

Academic Editor(s): Julio A. Seijas

Published: 15 November 2022

Publisher's Note: MDPI stays neutral with regard to jurisdictional claims in published maps and institutional affiliations.



Copyright: © 2022 by the authors. Submitted for possible open access publication under the terms and conditions of the Creative Commons Attribution (CC BY) license (<https://creativecommons.org/licenses/by/4.0/>).

1. Introduction

Conducting polymers are significantly used as electrochemically active materials for development of the electrode materials for supercapacitors [1,2]. PIN and correlated polymers have accepted emergent notice over decades for methodical and bioengineering purposes [3]. PIN themselves are affected with stumpy electrical and electrochemical conductivity; but has widespread considered as prophetic material due to its synthesis ease, cheapness, light weight, flexibility, thermal stability, tuneable conductivity, environmental stability, quick charge–discharge property [4] that can be regulated by doping and potential blending property confer them better to be exploited as a good challenger. Amendment of PIN through doping with metal oxides [5], metals, macrocyclic complexes, [12,14,15] has been of vital significance to afford the polymer composites for potential applications in chemical sensors [6], electrocatalytic [13], optical [16], sensitivity [8], bioengineering [7] and electrochemical energy storage [9–11]. PIN has recently been employed along with naturally abundant metal derivatives to achieve the materials with sustainable supercapacitance. In this perspective, macrocyclic Hb-functionalized PIN were used as material in the development of supercapacitors.

Hb is porphyrin-originated haeme complex with distinguished commercial accessibility, high stability, capability rate, and judicious price. Recently, heme proteins immobilized metal based electrodes showed interesting electrochemical behavior and greater charge/discharge cycling stability [9,17]. These properties prompts to utilize Hb as dopant to develop the PIN-based HPC for potential appliance in the development of working

electrodes for supercapacitors. Organophilic features of polymer globin chain connected with haeme assist bonding of Hb with matrix of conducting polymers to dispense the HPC with improved thermal stability, anti corrosive properties and enhanced supercapacitance.

Processing of materials through benign methods offers substantial industrial potential and viable feasibility. The present analysis deals with development of an environmentally gentle process of HPC through surfactant-assisted in-situ polymerization of indole (IN) in the presence of Hb(1% *w/w*) concentration. The implication of Hb as distinctive dopant for PIN, which results in high specific capacitance of HPC with microscopy characteristics, improved thermal stability and anticorrosive properties. These results of the proposed composite would be utilized to work further in the field of supercapacitors. The current research reflects its usefulness towards economically viable development of electrode material for electrochemical supercapacitors.

2. Experimental

2.1. Starting Materials

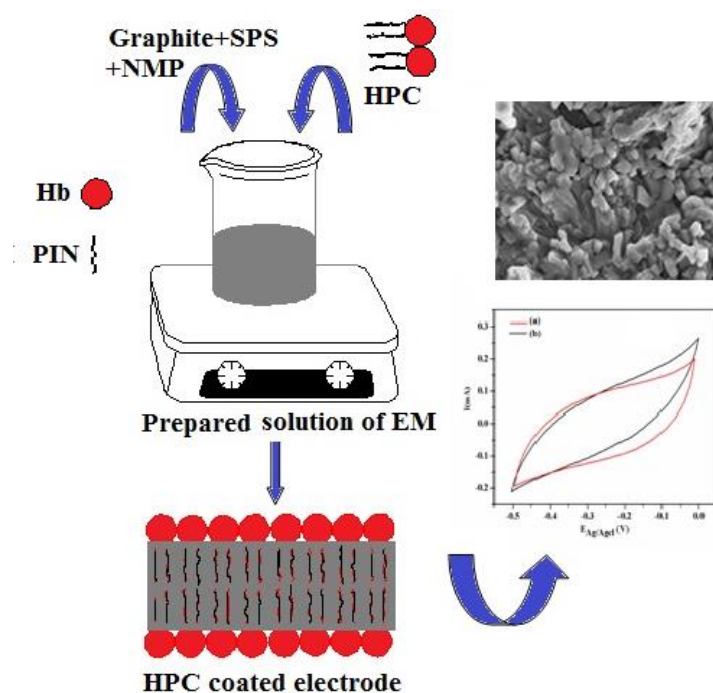
Commercially accessible Hb (Otto Kemi, India), indole (IN, SD Fine Chemicals), cetyltrimethylammoniumbromide CTAB ($\geq 99\%$) and graphite ($\geq 98.0\%$) were purchased from Otto Chemicka-Biochemica. Other chemicals and solvents were of AR grade. All chemicals and solvents were devoid of further purification. Sulphonated polysulphone (SPS) was synthesized and characterized according to the route accounted [15].

2.2. Synthesis of HPC

A sequence of HPC for improvement of supercapacitor electrodes was synthesized by the given procedure as illustrated earlier. The route of synthesis was accomplished through CTAB ($1.15\text{ g}, 3.50 \times 10^{-3}\text{ mol dL}^{-1}$)-assisted dilute solution polymerization of IN (0.12 mol dL^{-1}) in the presence of ferric chloride ($\text{FeCl}_3\text{ }30\text{ mL}, 1.85 \times 10^{-2}\text{ mol dL}^{-1}$) along with essential concentrations of Hb 1% (*w/w*). The contents were under mechanical stirring at the rate of 500 rpm over 24 h at $30 \pm 1^\circ\text{C}$. HPC was obtained through centrifugation at 3000 rpm over 20 min, followed by filtration, washing and drying at $50 \pm 1^\circ\text{C}/400\text{ mmHg}$ for over 5 h. PIN was also synthesized under identical reaction conditions and served as the control [16,17].

2.3. Fabrication of Working Electrodes

The working electrodes material (EM) was prepared by mixing an electroactive material (0.65 gm), graphite (0.10 gm) and SPS (5 g dL^{-1}) in *N*-methyl pyrrolidone (NMP). The content were blended and ultrasonicated for 15 min. The subsequent slurry was pressed on a stainless steel (SS) substrate which works as a current collector and left overnight at ambient temperature, pursue by $50^\circ\text{C}/400\text{ mmHg}$ for 24 h. This has afforded working electrodes with concluding thickness of electroactive materials over SS electrode was achieved to $0.05 \pm 0.01\text{ mg}$ [Scheme 1]. The electrodes were tested after 24 h of fabrication.



Scheme 1. Coating of SS with HPC to developed working electrode.

2.4. Material Characterization and Analysis Conditions

SEM of the gold-coated specimens was performed on a Hitachi S 3700 N at a primary beam voltage of 15 kV. For this purpose, the electrodes were prepared via the above-mentioned procedure. The scales of SEM images were between 10 and 30 μm . The corresponding magnifications ranged from 5.5 to 1.0 \times . TG-DTA-DTG was performed on an EXSTAR TG 6300 with sample weight ranging from 2.16 to 6.64 mg under N_2 at the rate of 30 mL min^{-1} from ~ 20 to 800 $^\circ\text{C}$.

All the electrochemical characterizations were made over the electrodes prepared for supercapacitor applications. Electrodes were electrochemically characterized in KOH (1.0 M) using a three-electrode cell assembly. Ag/AgCl was used as a reference electrode. Pt foil with a 1 cm^2 area was used as a counter electrode. A commercially available SS electrode served as a working electrode. Cyclic voltammetry (CV) was conducted at current compliance of 1 mA in the range of -0.5 – 0.0 V at 0.1 Vs^{-1} . All the measurements were performed at room temperature. Specific capacitance (C_s) of the electroactive material was calculated from the voltammetric charges by the CV curve, by means of the below relation:

$$C_s = \frac{q_a + |q_c|}{2m\Delta V}$$

where q_a and q_c are the voltammetric charges on anodic and cathodic scans in the capacitive potential region (ΔV) and m being the mass of active material.

3. Results and Discussion

3.1. Thermal Properties

The thermal characteristics of PIN and HPC have been investigated through simultaneous TG-DTA-DTG [Figure 1a,b]. The Thermal data has been expressed in terms of TG onset and endset, DTA and DTG peak temperatures ($^\circ\text{C}$). Prior to first step decomposition, the weight losses in the samples may attribute to the expulsion of moisture and residual solvents. The weight residue (W_r) corresponding to TG was expressed as % w/w . DTA signals and rate of degradation of samples in DTG are expressed as μV and mg/min respectively. The heat of fusion data revealed through DTA has been expressed in J/mg .

PIN shows two steps decomposition. The first step decomposition was emerged corresponding to TG onset at 201 leaving W_r 94.9. This has been sustained with a weak DTA

signals at 39.3 with corresponding peak temperature at 309. DTG reveals the decomposition of PIN at the rate of 0.16 with peak temperature at 245. The second step decomposition of PIN was appeared at 398 leaving Wr 69.3. This has been supported with an intense DTA signal at 0.46×10^{-3} with peak temperature 452 and the DTG peak temperature at 428 with rate of degradation 2.40×10^3 . The heat of fusion of PIN corresponding second step of decompositions was 7.69 [18–20] [Figure 1a].

The HPC derived through modification of PIN with Hb at (1%, *w/w*) shows two step decomposition. The first step decomposition of was appeared corresponding to TG onset at 207 leaving Wr 95.0. This has been supported with a broad DTA signal ranging 21.5 to 42.4 with corresponding at peak temperature ranging 280 to 323. DTG reveals the decomposition at the rate of 0.17 with peak temperature at 256. The second step disintegration of HPC was appeared at 411 leaving Wr 63.2. This has been sustained with an intense DTA signal at 404.3 at peak temperature 461 and the DTG peak temperature at 434 with rate of degradation 2.43. The endset temperature of decomposition was appeared at 456 with Wr 4.2. The heat of fusion of HPC corresponding second step of decomposition was 4.66 [Figure 1b]. Thus, due to the existence of Hb, the HPC was liable for high-thermal stability distinguishes with the PIN.

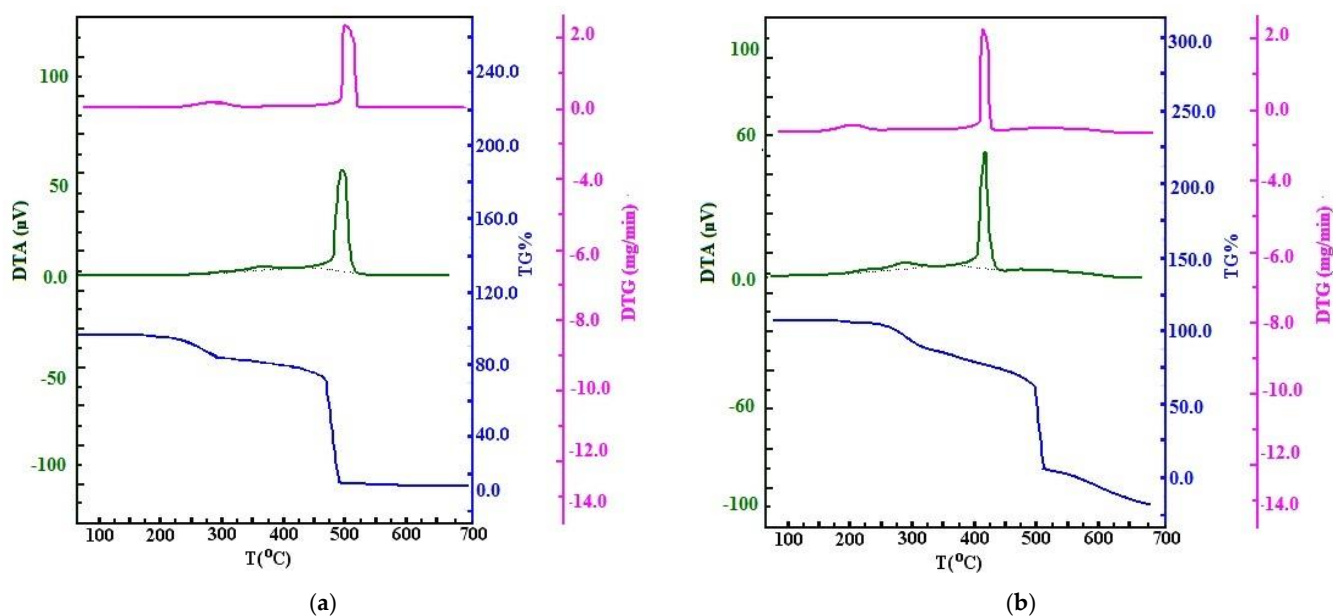


Figure 1. TG–DTA–DTG curves of (a) PIN (b) HPC.

3.2. Cyclic Voltammetry

The electrochemical performance of PIN and respective HPC electrodes synthesized at Hb concentrations 1% (*w/w*) has been investigated for electrochemical supercapacitors. The materials correspond to CV curves close to a rectangular contour in the voltage range of -0.5 – 0.0 V at scan rates of 0.01Vs^{-1} in 1.0 M KOH and there is no current peak source by a redox reaction, demonstrating a typical capacitive behaviour with good charge propagation of these materials. PIN and respective HPC (1%), the C_s (Fg^{-1}) of electrodes has been 21.60 and 39.40 respectively [Figure 2a] [9,21]. The sturdy escalation in specific capacitance with mounting fraction of Hb in the matrix of the polymer was monitored in the HPC. Electrochemical studies on PIN and HPC confer exhilarating outcomes which reveal that HPC is capable material for preparation and its growth as a material for energy storage devices.

The EIS spectra were represented through Nyquist plot to study the stability or any loss in the protective properties of the coating over the SS surface in KOH (1.0 M). It executes to establish the parameters for electron transfer reactions at the interface of the

working electrode. EIS spectra of PIN and HPC (1% w/w) were considered in the frequency ranges from 0.1 to 1000 Hz with pulse amplitude of 0.03 mV. Nyquist diagram for the PIN and HPC1% electrodes are shown in [Figure 2b]. The electrodes contain two parts, one is linear part at low frequency region and another illustrates quasi semicircle in the high frequency region. The electrolyte resistance (R_s), can be instigated from the half circle interception point on the real axis while the charge transfer resistance (R_{ct}), was analysed by measuring the scale of the diameter of semicircle on the electrode surface. PIN exemplifies elevated impedance values distinguish with those achieved for the HPC. The curves for HPC also showed a divergence in slope from an erect location in relative to PIN, which is attributed to the low R_{ct} values and may be assigned to the high mobility and porosity within the electrodes. This maintains electronic transfer in the HPC, thus significantly dipping the R_{ct} value, making it further capacitive. The augment in electron transport in HPC is probably the charge transfer between Hb and PIN. Due to the enormous surface area of Hb, may provide as connecting PIN and results in higher conductivity, thus lowering the R_{ct} values obtained for HPC. The R_s and R_{ct} for HPC is less than the PIN, which concludes that HPC is vastly conductive as well as moderately stable as an electrode material [22,23].

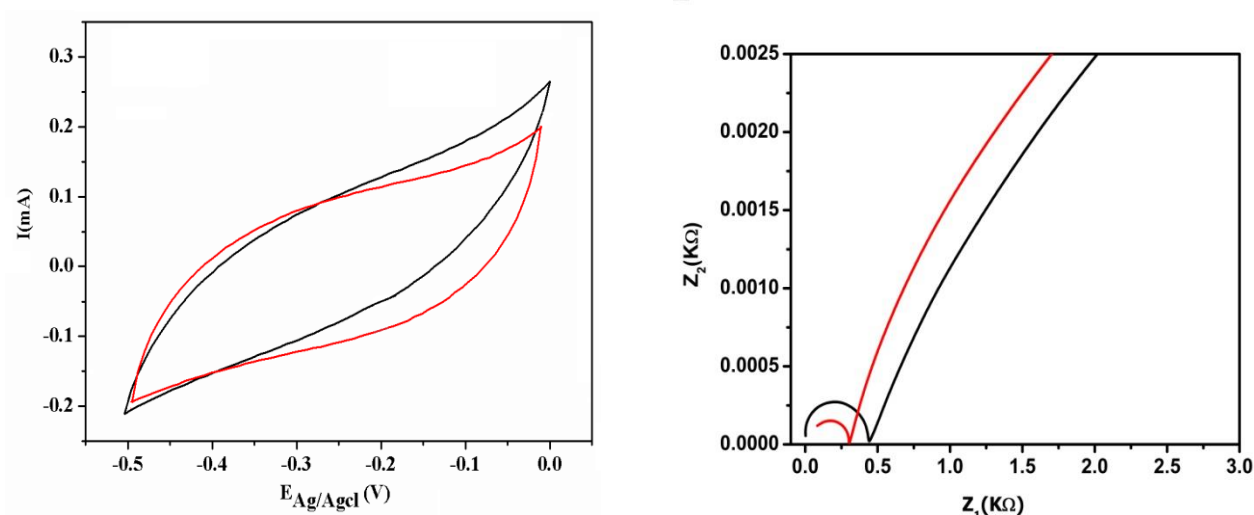


Figure 2. CV of (a) PIN (red) and (b) HPC (1% black) at scan rate (Vs^{-1}) with reference to Ag/AgCl and Nyquist plot of PIN (red) and HPC (1% black) in KOH.

3.3. Corrosion Analysis

The corrosion protective performance of PIN and HPC over the SS substrates in a 1.0 M KOH solution was investigated as a function of immersion time through Potentiodynamic Polarization measurements

3.3.1. Potentiodynamic Polarization Measurements

The extent of corrosion inhibition ability of PIN and HPC coatings deposited over SS substrate has been investigated through the Tafel plot. The electrochemical data has been presented in terms of E_{corr} (V), I_{corr} (Acm^{-2}) and CR ($mm\ year^{-1}$) under potentiodynamic conditions from $-1.0V$ to $1.0V$, $0.1Vs^{-1}$ at room temperature. The more negative E_{corr} and the larger I_{corr} usually correspond to faster corrosion rates while the more positive E_{corr} and the smaller I_{corr} mean a slower corrosion process. Extrapolation of anodic and cathodic Tafel lines is one of the most popular DC techniques for charge transfer controlled reactions estimating the corrosion rate [24]. It was observed from the polarization curve, the bare stainless steel (SS) electrode shows E_{corr} $-1.27\ V$ and I_{corr} 1.90×10^{-4} (Acm^{-2}) which corresponds to faster corrosion rate. The PIN coating shows the E_{corr} $-0.77\ V$ and

$I_{\text{corr}} 1.19 \times 10^{-4}$ (Acm^{-2}) compared to HPC shows a more positive shift ranging $E_{\text{corr}} -0.63$ V and decreased $I_{\text{corr}} 1.85 \times 10^{-5}$ (Acm^{-2}) at scan rate 0.1 Vs^{-1} . Thus, the comparative results of SS, PIN and HPC shows in Table 1. The HPC exhibited the good anticorrosion activity as compared to PIN [25,26].

Table 1. Corrosion parameters (E_{corr} , I_{corr} , R_p , CR) obtained from Tafel plots of bare SS electrode, PIN and HPC(1%).

Substrate	E_{corr} (V)	I_{corr} (Acm^{-2})	R_p (Ohm)	CR (mm yr^{-1})
Stainless Steel (SS)	-1.27	1.90×10^{-4}	1.22×10^{-2}	6.219
PIN	-0.77	1.19×10^{-4}	6.48×10^{-2}	0.389
HPC(1%)	-0.63	1.82×10^{-5}	1.28×10^4	0.059

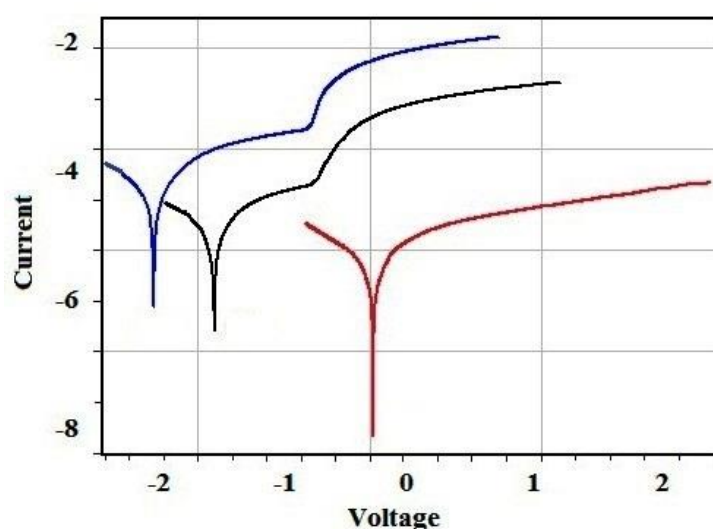


Figure 3. Tafel plot @0.1(a) stainless steel (blue), (b) PIN (green) and (c) HPC(red) (1%) in KOH.

3.3.2. Microstructure

In order to have further insight into the effect of Hb on the stability, the SEM images has been recorded before and after polarization experiments [Figure 4]. All SEM investigations have been conducted over the supercapacitors electrodes fabricated according to the procedure reported. The electrode derived from PIN shows granular morphology. The morphology of HPC electrode was maintaining to rod shape even in presence of Hb emerged into flaky morphology [27].

However, the SEM images of the electrodes derived from PIN and representative HPC indicate significant changes in the morphology after the polarization experiments. Pits were clearly seen in the PIN electrode. The flaky morphology of HPC was changed from rod shaped to phase separated morphology, there is no pitting corrosion at the surface but swelling occurs with no sign of degradation. This is a usual phenomenon of the delaminating of coating of polymer observed under polarization experiments. The results suggest that the incorporation of Hb improves the corrosion protective performance of the coatings over their underlying substrates in the KOH.

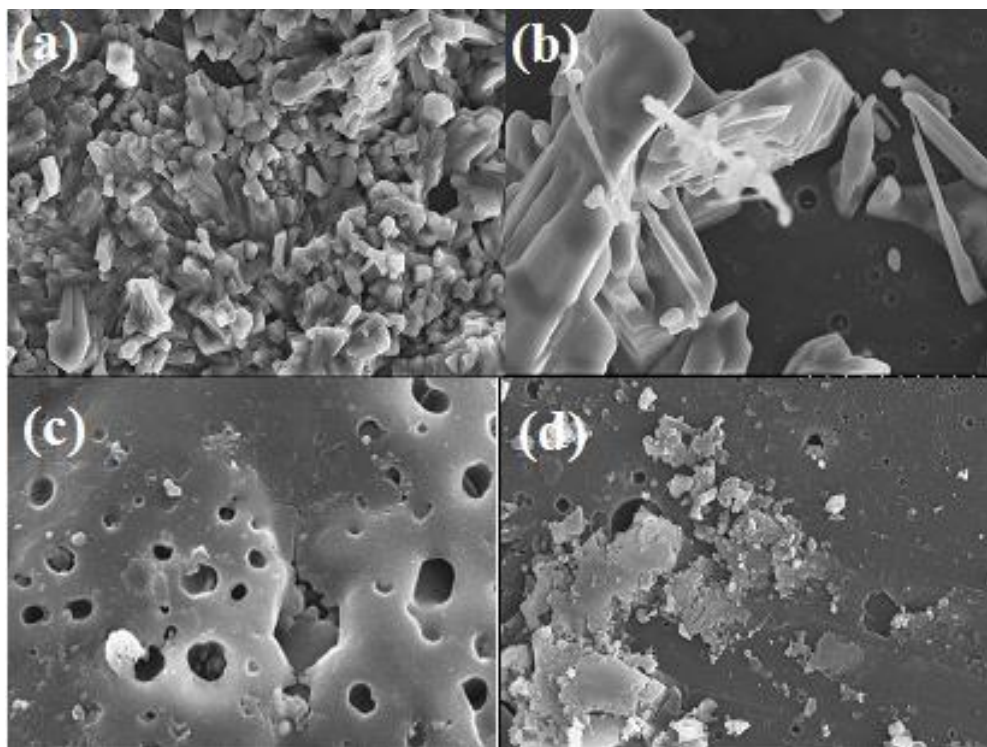


Figure 4. SEM images of (a) PIN and (b) HPC before recording polarization experiment (c) PIN and (d) HPC SEM images after recording polarization experiment in KOH.

4. Conclusions

Development of HPC for supercapacitor electrodes were through CTAB ($1.15 \text{ g}, 3.50 \times 10^{-3} \text{ mol/dL}$) assisted dilute solution polymerization of IN (0.12 mol/dL) in presence of FeCl_3 ($30 \text{ mL}, 1.85 \times 10^{-2} \text{ mol/dL}$) at concentration of Hb ($1\%, w/w$) at $30 \pm 1 \text{ }^\circ\text{C}$ over 24 h. The formation of HPC was ascertained through SEM and TG–DTA–DTG analysis. From thermal analysis, PIN and HPC shows two step decompositions which onset from 201 to $398 \text{ }^\circ\text{C}$ and 207 to $411 \text{ }^\circ\text{C}$. Hence, it can be concluded that incorporation of Hb in PIN steadily increases its thermal stability. PIN and respective HPC (1%), the C_s (Fg^{-1}) of electrodes has been 21.60 and 39.40 respectively. The rise in specific capacitance with incorporation of Hb in the matrix of the PIN was examined in the HPC. The R_s and R_{ct} for HPC is less than the PIN, which conclude that HPC is immensely conductive as well as judiciously stable as an electrode material. PIN and HPC shows granular and rod shape morphology which changes to phase separated morphology. Thus SEM based observations indicate that after the polarization experiments; the surface of the electrodes has been tarnished but the incorporation of Hb improves the corrosion protective performance of HPC coating. Present finding has been made and open new avenues for the fabrication of a new generation of supercapacitors.

Funding: This research received no external funding.

Acknowledgments: The author would like to thank CSIR, India, for awarding JRF/SRF and Department of Chemistry, GBPUA&T for laboratory facility. Author is thankful to the Govt. P.G. College, Kashipur and Director, Higher Education, Govt. of Uttarakhand, for providing facilities.

Conflicts of Interest: The author declares no conflict of interest.

References

1. Akinwolemiwa, B.; Peng, C.; Chena, G.Z. Redox electrolytes in supercapacitors. *J. Electrochem. Soc.* **2015**, *162*, 5054–5059.
2. Chen, S.M.; Ramachandran, R.; Mani, V.; Saraswathi, R. Recent advancements in electrode materials for the high performance electrochemical supercapacitors: A review. *Int. J. Electrochem. Sci.* **2014**, *9*, 4072–4085.
3. Ramya, R.; Sivasubramanian, R.; Sangaranarayanan, M.V. Conducting polymers-based electrochemical supercapacitors—progress and prospects. *Electrochim. Acta.* **2013**, *101*, 109–129.

4. Wang, L.; Li, X.; Yang, Y. Preparation, properties and applications of polypyrroles *React. Funct. Poly.* **2001**, *47*, 125–139.
5. Sahyar, B.Y.; Kaplan, M.; Ozsoz, M.; Celik, E.; Otlis, S. Electrochemical xanthine detection by enzymatic method based on Ag doped ZnO nanoparticles by using polypyrrole. *Bioelectrochem.* **2019**, *130*, 107327.
6. Paul, S.; Amalraj, F.; Radhakrishnan, S. CO sensor based on polypyrrole functionalized with iron porphyrin. *Synth. Met.* **2009**, *159*, 1019–1023.
7. Balint, R.; Cassidy, N.J.; Cartmell, S.H. Conductive polymers: Towards a smart biomaterial for tissue engineering. *Acta Biomater.* **2014**, *10*, 2341–2353.
8. Geng, L.; Wang, S.; Zhao, Y.; Li, P.; Zhang, S.; Huang, W.; Wu, S. Study of the primary sensitivity of polypyrrole/r-Fe₂O₃ to toxic gases. *Mater. Chem. Phys.* **2006**, *99*, 15–19.
9. Khairy, M.; El-Safty, S.A. Hemoproteins–nickel foam hybrids as effective supercapacitors. *Chem Commun.* **2014**, *50*, 1356–1358.
10. Ghosh, S.; Maiyalagan, T.; Basu, R.N. Nanostructured conducting polymers for energy applications: Towards a sustainable platform. *Nanoscale.* **2016**, *8*, 6921–6947.
11. Baghayeri, M.; Zare, E.N.; Lakouraj, M.M. Monitoring of hydrogen peroxide using a glassy carbon electrode modified with hemoglobin and a polypyrrole-based Nanocomposite. *Microchem. Acta* **2015**, *182*, 3–4.
12. Jinchun, T.; Nan, L.; Qing, Y.; Rui, W.; Wangchang, G.; Yanjuan, L.; Tong, Z.; Xiaotian, L. Humidity-sensitive property of Fe²⁺ doped polypyrrole. *Synth. Met.* **2009**, *159*, 2469–2473.
13. Zhou, Q.; Li, C.M.; Li, J.; Cui, X.; Gervasio, D. Template-synthesized cobalt porphyrin/polypyrrole nanocomposite and its electrocatalysis for oxygen reduction in neutral medium. *J. Phys. Chem. C.* **2007**, *111*, 11216–11222.
14. Basavaraja, C.; Kim, N.R.; Jo, E.; Pierson, R.; Huh, D.S.; Venkataraman, A. Transport properties of polypyrrole films doped with sulphonic acids. *Bull. Kor. Chem. Soc.* **2009**, *30*, 2701–2706.
15. Unnikrishnan, L.; Madamana, P.; Mohanty, S.; Nayak, S.K. Polysulfone/C30B Nanocomposite Membranes for Fuel Cell Applications: Effect of Various Sulfonating Agents. *Polym. Plast. Technol. Eng.* **2012**, *51*, 568–577.
16. Wadkar, N.S.; Waghuley, S.A. Complex optical studies on conducting polyindole as synthesized through chemical route. *Egypt. J. Basic Appl. Sci.* **2015**, *2*, 19–24.
17. Dessy, A.; Piras, A.; Schir, A.G.; Levantino, M.; Cupane, A.; Chiellini, F. Hemoglobin loaded polymeric nanoparticles: Preparation and characterizations. *Eur. J. Pharm. Sci.* **2011**, *43*, 57–64.
18. Abthagir, P.S.; Saraswathi, R. Charge transport and thermal properties of polyindole, polycarbazole and their derivatives. *Thermochim. Acta.* **2004**, *424*, 25–35.
19. Unal, H.I.; Sahan, B.; Ozlem, E. Investigation of electrokinetic and electrorheological properties of polyindole prepared in the presence of a surfactant. *Mater. Chem. Phys.* **2012**, *134*, 382–391.
20. Rajasudha, G.; Shankar, H.; Thangadurai, P.; Boukos, N.; Narayanan, V.; Stephen, A. Preparation and characterization of polyindole–ZnO composite polymer electrolyte with LiClO₄. *Ionics.* **2010**, *16*, 839–848.
21. Khairy, M.; El-Safty, S.A. Promising supercapacitor electrodes based immobilization of proteins onto macroporous Ni foam materials. *J. Energy Chem.* **2015**, *24*, 31–38.
22. Mansfeld, F. Use of electrochemical impedance spectroscopy for the study of corrosion protection by polymer coatings. *J. Appl. Electrochem.* **1995**, *25*, 187–202.
23. Liu, X.W.; Xiong, J.P.; Lv, Y.W.; Zuo, Y. Study on corrosion electrochemical behavior of several different coating systems by EIS. *Prog. Org. Coat.* **2009**, *64*, 497–503.
24. Mondal, J.; Marandi, M.; Kozlova, J.; Merisalu, M.; Niilisk, A.; Sammelselg, V. Protection and functionalizing of stainless steel surface by graphene oxide-polypyrrole composite coating. *Chem. Chem. Eng.* **2014**, *8*, 786–793.
25. Dündükcü, M.; Yazici, B.; Erbil, M. The effect of indole on the corrosion behaviour of stainless steel. *Mater. Chem. Phys.* **2004**, *87*, 138–141.
26. Alejandra, C.A.; Valderrama, R.C.; Martinez, J.A.; Vargas, A.E.; Salazar, S.G.; Barcena, M.S.; Casillas, N. Corrosion of Aluminium, Copper, Brass and Stainless Steel 304 in Tequila. *Int. J. Electrochem. Sci.* **2012**, *7*, 7877–7887.
27. Gupta, B.; Chauhan, D.S.; Prakash, R. Controlled morphology of conducting polymers: Formation of nanorods and microspheres of polyindole. *Mater. Chem. Phys.* **2010**, *120*, 625–630.